Journal of Volcanology and Geothermal Research 430 (2022) 107626

Contents lists available at ScienceDirect

Journal of Volcanology and Geothermal Research

journal homepage: www.journals.elsevier.com/journal-of-volcanology-and-geothermal-research

The new lava dome growth of Nevado del Ruiz (2015–2021)

Milton Ordoñez [a,*], Carlos Laverde [b], Maurizio Battaglia [c,d]

[a] Colombian Geological Survey, Volcanological and Seismological Observatory of Manizales, Ave 12 de octubre No. 15-47, Manizales, Caldas, Colombia
[b] Colombian Geological Survey, Volcanological and Seismological Observatory of Pasto, Calle 27 N° 9 ESTE - 25, Barrio La Carolina, Pasto, Colombia
[c] U.S. Geological Survey, Volcano Disaster Assistance Program, Moffet Field, CA 94035, USA
[d] Department of Earth Sciences, Sapienza – University of Rome, P.le A. Moro 5, 00185 Rome, Italy

ARTICLE INFO

Keywords:
Nevado del Ruiz
Crater morphology
Dome forming eruption
Mathematical modeling

ABSTRACT

The morphology of the summit of Nevado del Ruiz volcano (Colombia) and its active Arenas crater is the product of complex interactions between effusive and explosive eruptions, and the dynamics of the summit glacier. Here, we document the morphologic evolution of the summit of Nevado del Ruiz, and the growth of its dome, from a variety of methods: monitoring data (2010 to 2021), photogrammetry, remote sensing, and quantitative modeling. The present morphology of Arenas crater, with small terraces limited by the walls of the crater, various vents of ash emission, and zones of fumarolic activity, has been shaped by the activity following the eruptions of 1845, 1985, 1989, 2012 and the volcanic unrest of the last 10 years. The latest emplacement of a lava dome at the bottom of the main crater began in 2015. The dome grew, with fluctuations in its extrusion rate between ~0.19 m^3/s (November 2015) and 0.02 m^3/s (February 2018), until December 2019, reaching a diameter of ~130 m, a maximum height of ~60 m, and a volume of $1.7 \pm 0.2 \times 10^6$ m^3.

1. Introduction

Nevado del Ruiz (Fig. 1), part of the North Volcanic Segment of Colombia (NVSC), is the most active volcano in Colombia. The volcano produces calk-alkaline dacite and andesite lavas typical of the South American active continental margins. Its eruptions produce lava flows, pyroclastic density currents, tephra, and ash falls, and generate lahars (Ceballos et al., 2020a).

The Volcanological Observatory of Colombia (now Volcanological and Seismological Observatory of Manizales, Colombian Geological Survey – SGC-OVSM) started a monitoring program of the crater morphology in April 1986, with the support of the Colombian Air Force. The monitoring is based on the analysis of topographic sketches and maps, aerial and terrestrial photographs, satellite and radar images, and digital elevation models (DEMs). Since 2015, the SGC-OVSM had limited success in employing military (Colombian Air Force), commercial, and drone flights to monitor changes in the topography of the summit of the volcano. The elevation of the Nevado del Ruiz summit is at 5321 m a.s.l., and strong winds, cloud cover, and strong gas emissions commonly prevent observations of the crater. Only two military planes and one drone successfully flew over the summit to capture aerial photographs of Arenas crater and the new lava dome.

Nevado del Ruiz overlies the north-northeast Palestina fault, which is a major tectonic element of the Central Cordillera of Colombia (Fig. 1). The Termales-Villamaría fault crosses Nevado del Ruiz in the southeast - northwest direction (Fig. 1). The summit of the Nevado del Ruiz is practically flat and covered by a glacier of about 8.4 km^2 (Ceballos et al., 2020b). Erosion, induced by the retreat of the summit glacier, is changing the morphology of the summit, and re-shaping the canyons and headwaters draining the volcano (Ceballos et al., 2020b). Streams descending the edifice flow to the east into the Gualí, Azufrado, Lagunilla, and Recio rivers which drain into the Magdalena River; and flow to the west into the Molinos, Nereidas, Río Claro and Chinchiná rivers draining into the Cauca River. Arenas crater currently has an almost circular morphology with three inner and semicircular terraces (upper, middle, and lower) separated by three steps. Activity occurs in the lower zone (the bottom of the crater) and features two open vents and various areas of fumaroles. Because of erosion, at present, Arenas crater has a diameter of 980 m in the southwest-northwest direction, 870 m in the southeast-northeast direction and a depth of 300 m (Figs. 1, 4 and 5).

Nevado del Ruiz entered a new eruption cycle in 2012, after 11 years of quiescence and 27 years after the tragic eruption of November 13, 1985, that destroyed the town of Armero and some neighborhoods of the town of Chinchiná (Voight, 1990). Precursory aseismic deflation was

* Corresponding author.
E-mail addresses: mordonez@sgc.gov.co (M. Ordoñez), claverde@sgc.gov.co (C. Laverde), mbattaglia@usgs.gov (M. Battaglia).

https://doi.org/10.1016/j.jvolgeores.2022.107626
Received 9 November 2021; Received in revised form 11 July 2022; Accepted 14 July 2022
Available online 16 July 2022

observed between 2009 and late 2011 (Ordoñez et al., 2015). Between January and February 2012, seismicity increased, the volcano had several small ash emissions and inflation began. Seismic activity, deformation, SO_2 release and ash emissions increased significantly until May 2012. Two small explosive eruptions (VEI = 1) occurred on May 29 and June 30, 2012, clearing the volcanic conduit, and opening the system. After these eruptions, the activity remained constant with high seismicity, inflation, and intermittent emission of water vapor, SO_2 and ashes as potential indicators of magma migration (Servicio Geológico Colombiano, 2012). Short and sporadic 'drumbeat' seismic episodes started in August 2015 coinciding with explosions and a dome-forming eruption at the bottom of the main crater (Servicio Geológico Colombiano, 2015). The dome grew, with fluctuations in its extrusion rate, until December 2019, reaching a diameter of ~130 m, a maximum height of ~60 m and total volume of $\sim 1.7 \pm 0.2 \times 10^6$ m^3. The Nevado del Ruiz lava dome can be considered a low type of lava dome according to the classification by Blake (1990) and Fink and Anderson (2000). Blake (1990) distinguishes four types of lava domes by their morphology, correlated to the yield strength of the magmas: upheaved plugs, Pelean domes, low lava domes and coulees.

Here we introduce monitoring data of the unrest and dome forming eruption from 2010 to 2021 and discuss a quantitative model of the summit dome extrusion. Finally, we make available in the Supplementary Material additional data collected by visual monitoring of Arenas crater and the summit dome from 1939 to 2010.

2. Methods

The SGC-OVSM has been actively monitoring the crater morphology and surface activity of Nevado del Ruiz volcano since April 1986. The 2015–2021 dome forming eruption was monitored by geodetic (GNSS, tilt) and seismic networks, geochemistry measurements, webcams, photogrammetry, and infrasound (Figs. 1 and 2). The availability of these data sets has allowed to obtain improved estimates of the surface area and volume of the lava dome and develop of quantitative models of the evolution of the dome forming eruption.

Until 2010 monitoring was mainly based on the analysis of terrestrial and aerial photographs taken during periodic visits to the crater and occasional flyover of the summit of the volcano with the support of the Colombian Air Force (Figs. 3 and 4).

These images allowed to produce topographic sketches and maps of the summit (Fig. 5), and infer the perimeter, diameter, and depth of the main crater. Photographs were also employed to observe changes in the morphology of the crater, ranging from minor features like terraces, secondary craters, cracks, fissures, fumaroles, to the evolution of the dome forming eruption (2015–2021).

Since 2010, qualitative observations of the morphology have been integrated by quantitative measurements from satellite (Fig. 6) and radar images, employed to produce digital elevation models (DEMs) of the summit.

Sentinel-2 satellite images (European Space Agency, Drusch et al., 2012) were used to identify thermal anomalies in the crater (Fig. 7), a sign of renewed activity during the dome forming eruption. TanDEM-X (TDX) and TerraSAR-X (TSX) images (German Aerospace Center, https://terrasar-x-archive.terrasar.com) allowed to check the evolution of the lava dome growth and estimate the rate of lava extrusion (Fig. 8).

To estimate the surface area and volume of the lava dome, we divided the dome in two sections: upper half and lower half (Fig. 9). For the upper half, the one above the bottom of the crater, we first scaled and georeferenced TDX and TSX images (Fig. 10). We chose the Planet Labs image of March 14, 2018, showing a clear view of the bottom of the crater, to calibrate the initial dimensions of the dome. These dimensions were assumed equivalent to the dimensions of the dome in the TDX image of April 9, 2018. Using this calibration, we estimated a pixel per meter factor and applied it to all the TDX and TSX images. Then we digitized a border polygon in each image to calculate the perimeter and

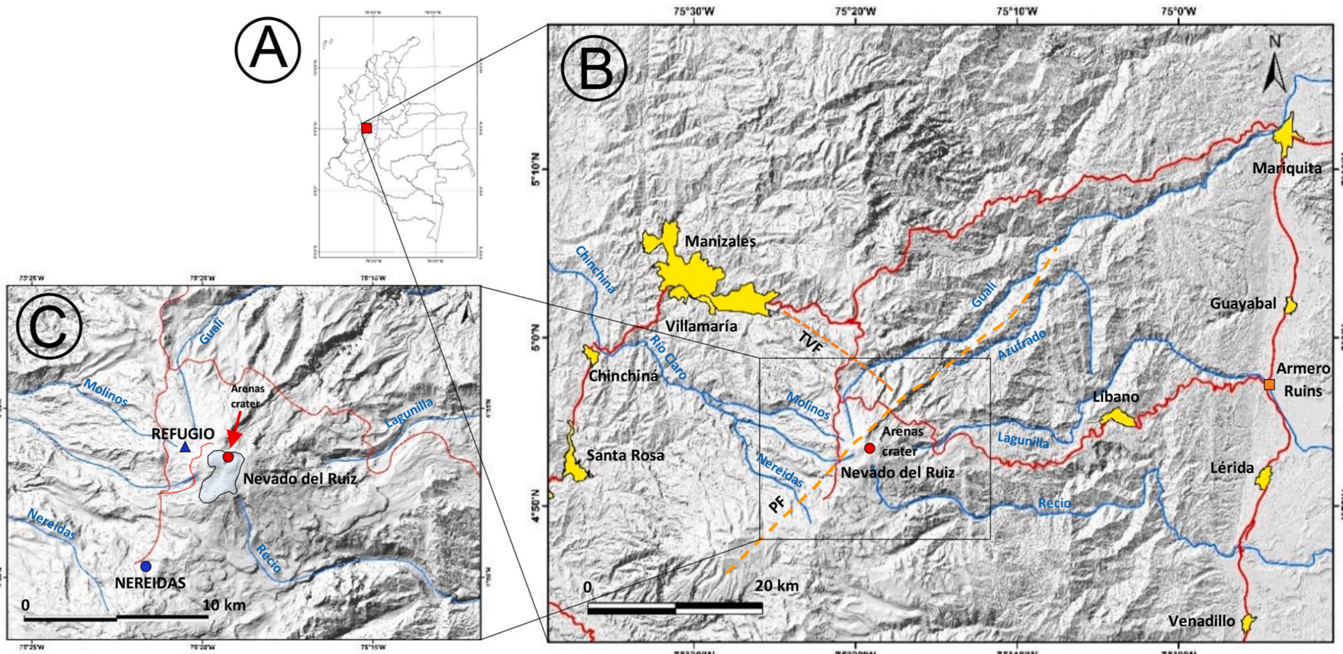

Fig. 1. (A) Map of Colombia with the location of the study area. (B) Location of Nevado del Ruiz volcano plotted on the NASA 90 m DEM (Jarvis et al., 2008; https://cgiarcsi.community/data/srtm-90m-digital-elevation-database-v4-1). Center of crater (Red circle): Latitude 4.982° N, longitude 75.319° W, elevation 5321 m a.s.l.; the volcano is in the Central Cordillera of Colombia, 28 km southeast of the city of Manizales, and 135 km west of the city of Bogota (Capital of Colombia). Red lines: access road to the volcano; Blue lines: main rivers; Yellow polygons: main towns; Orange dashed lines: Palestina fault (PF) and Termales-Villamaría fault (TVF); Orange square: Armero ruins. (C) Location of the proximal area of Nevado del Ruiz volcano. Red circle: Arenas crater located at the summit of the volcano surrounded by the glacier (light blue polygon); Blue triangle: REFUGIO tiltmeter station; Blue circle: NEREIDAS GNSS station. (For interpretation of the references to colour in this figure legend, the reader is referred to the web version of this article.)

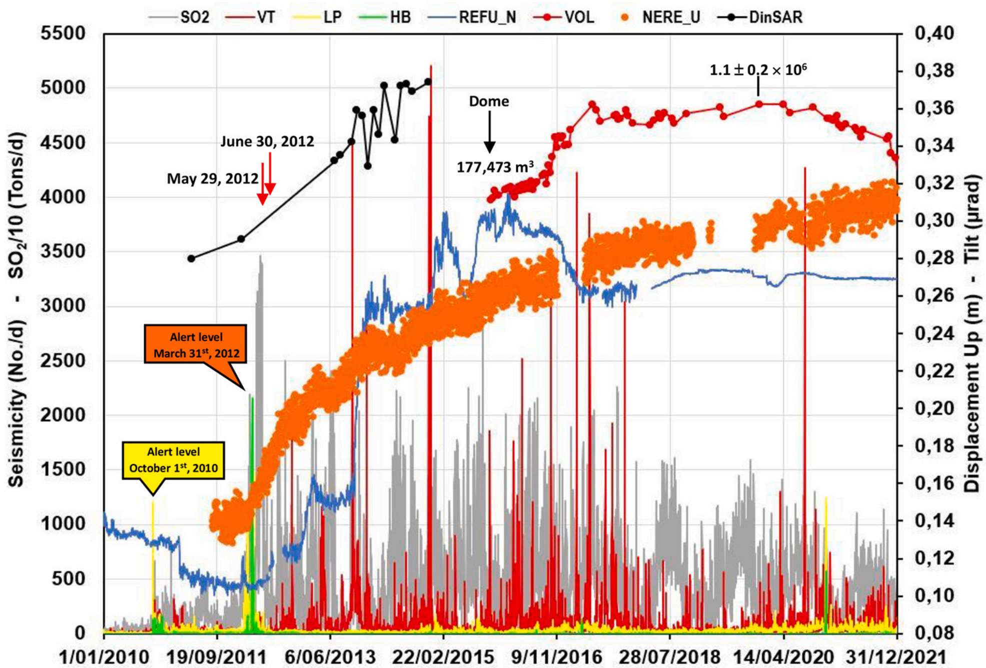

Fig. 2. Nevado del Ruiz. Time series of seismic, geodetic, and geochemical data from 2010 to 2021, acquired by the monitoring program of the OVSM. Grey line (SO2): SO_2 flux in tons/day; red line (VT): volcano-tectonic seismic events; yellow line (LP): long period seismic events; green line (HB): hybrid seismic events; blue line (REFU_N): north component of REFUGIO tiltmeter; orange dots (NERE_U): vertical displacement of the Global Navigation Satellite System (GNSS) station NEREIDAS; Black line and dots: Line Of Side (LOS) displacement based on DinSAR; red line and dots (VOL): lava dome volume (from $\sim 0.1 \times 10^6$ m^3 in November 2015 to $\sim 1.1 \times 10^6$ m^3 in December 2019); red arrows: eruptions; black arrow: beginning of lava dome emplacement.

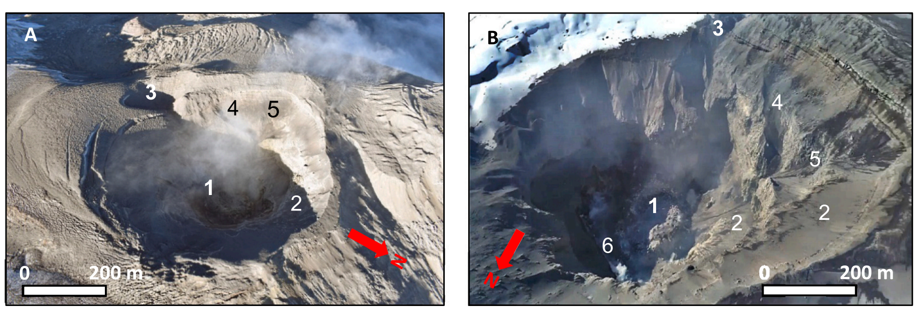

Fig. 3. Volcanic features of Arenas crater (Nevado del Ruiz). (A) View from the northeast (January 10, 2020); (B) View from the north (January 7, 2021) (image courtesy of Guillermo Sanchez). (1) Lava dome; (2) inner terraces; (3) southwest secondary crater, 150 m in diameter; (4) west fissure; (5) eroded northwest secondary crater; (6) fumarole zone around the dome. See also Figs. 4 and 5.

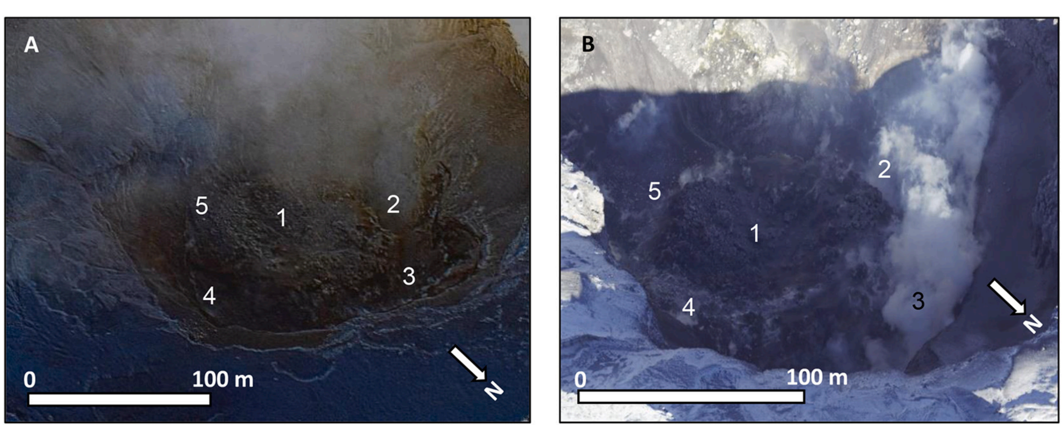

Fig. 4. Evolution of Arenas crater (Nevado del Ruiz). (A) January 10, 2020; (B) January 29, 2021 (image courtesy of Jeronimo Valencia). (1) Depression in the center of the dome, caused either by partial subsidence or cooling of the lava dome; (2) the new secondary crater with a diameter of approximately 15 m, located at the edge of the dome; (3, 4 and 5) several sources of gas/ashes emission located around the dome.

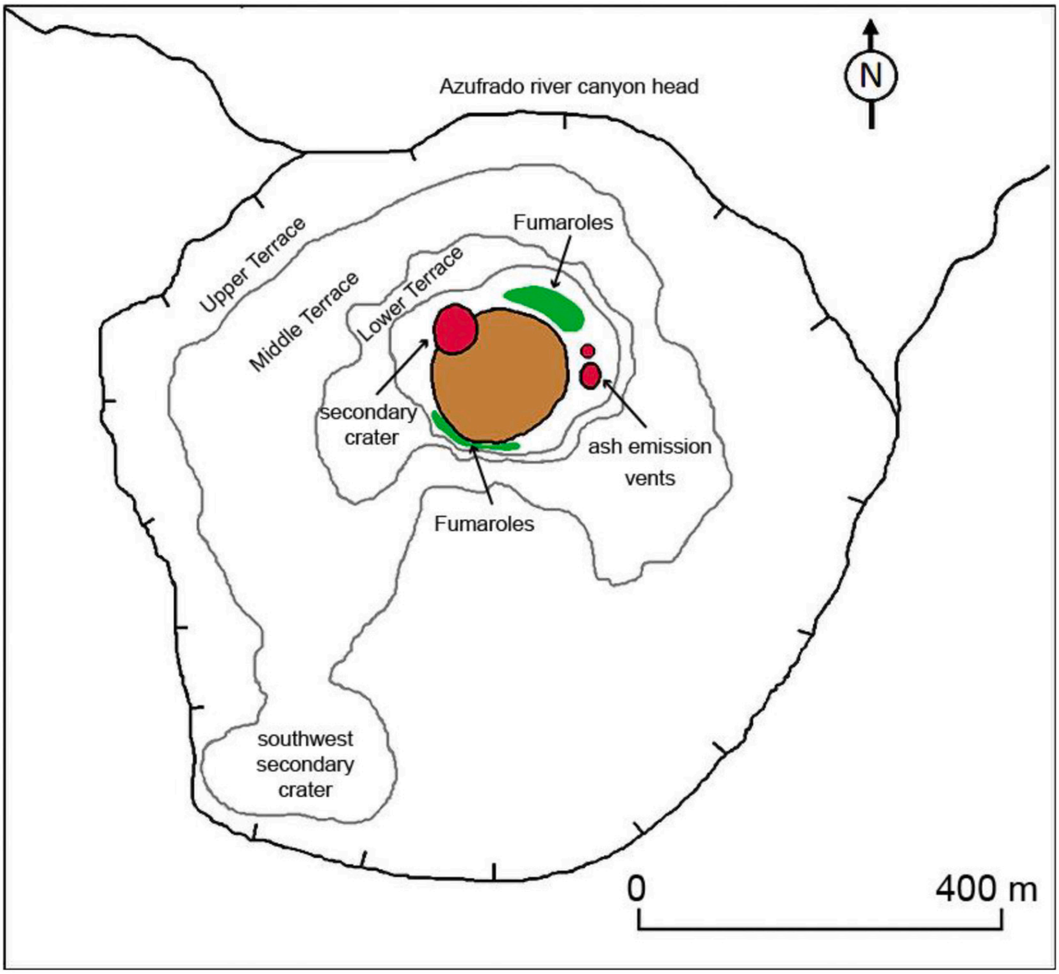

Fig. 5. Diagram of the Arenas crater in January 2020 based on the images in Figs. 3 and 4. The map shows the lava dome (in brown) at the bottom of the crater, various fumarolic zones located in the northeast and south edges of the dome, a secondary crater located on the northwest edge of the dome, and an ash emission zone located east of the dome's edge. (For interpretation of the references to colour in this figure legend, the reader is referred to the web version of this article.)

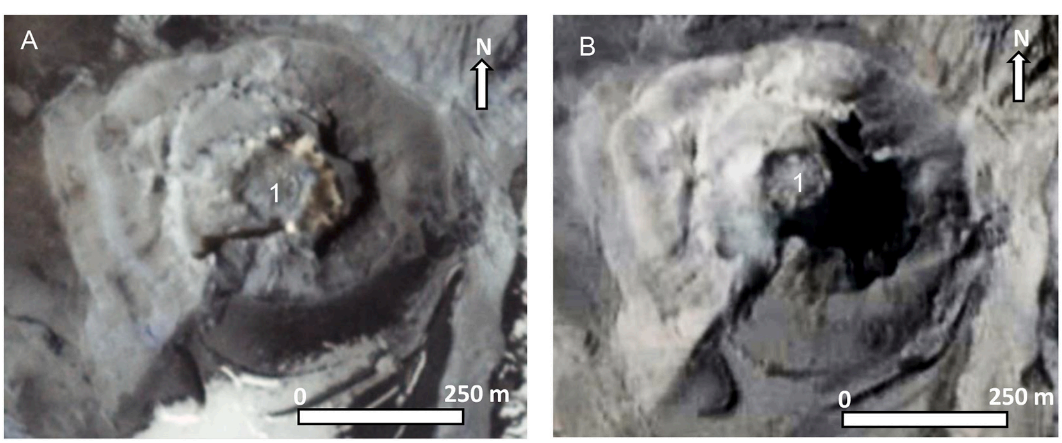

Fig. 6. Planet Labs satellite images of the Arenas crater showing the growth of the lava dome (labelled 1 in the images). (A) March 14, 2018. (B) January 10, 2020. Images courtesy of Planet Labs FBC, available online at https://www.planet.com.

the surface area of the dome. Finally, we estimated the height of the dome applying the formula for an oblate ellipsoid half-dome (Monolithic Dome Institute, 2001) to calculate the volume of the upper section of the dome (Kósik et al., 2015). The volume of the lower section of the dome was calculated using a plane located below the upper section in contact with different resolution DEMs of the Arenas crater. The total volume of the dome was obtained adding the volume of the upper and lower sections. The lava extrusion rate was estimated based on the periodical surface area and volume change, and calibrated with the minimum and maximum volume of the dome (Fig. 11).

Finally, we simulated the lava dome extrusion using the LAVA-C code (Richardson and Connor, 2014) through pulses of lava assuming

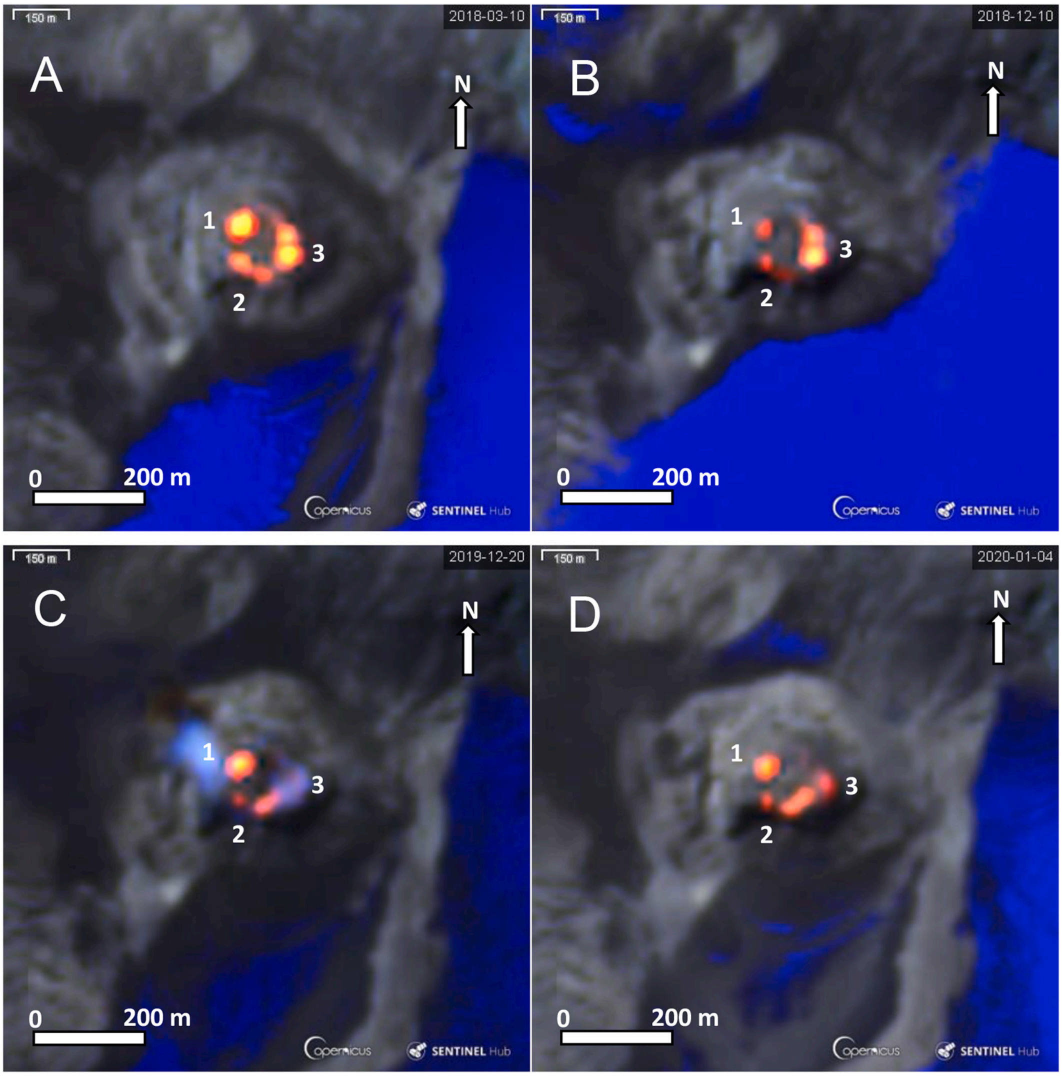

Fig. 7. Thermal images of the Arenas crater from the Sentinel-2 satellite (European Space Agency, (A) March 10, 2018; (B) December 10, 2018; (C) December 20, 2019; (D) January 4, 2020. The yellow and red colors represent the location of areas of high temperature, interpreted as (1) the secondary crater (northwest edge of the dome), (2) fumarolic zones (south), and (3) ash emission vents (east of the dome). See also Figs. 5 and 6. These images correspond to a spectral combination, sensitive to the temperatures inside the crater, of Sentinel-2 bands B12 (SWIR2), B11 (SWIR1) and B8 (NIR), where the combination's bands that show the coldest areas appear in blue and the hottest areas appear in yellow and red. (For interpretation of the references to colour in this figure legend, the reader is referred to the web version of this article.)

a semi-empirical relation between a reference thickness and the viscosity of the lava; and a DEM of the volcano's crater to estimate the changes in slope and constrain the thickness of the lava pulses (Fig. 12).

3. Dome forming eruption

In September 2010, seismicity, and emission of SO_2 increased (Fig. 2; INGEOMINAS, 2010), and on October 1st the alert level was changed from Green to Yellow (change in volcanic activity). Fifteen months later, in February 2012, the volcano started to inflate (Ordoñez et al., 2015) (Fig. 2), and in March 2012, the level of seismicity, discharge of water vapor (identified through the visual observations of the intensity of the white colour of the plume) and SO_2, and ash emissions increased again (Fig. 2; Servicio Geológico Colombiano, 2012). Because of this increase, the SGC-OVSM changed from Yellow to Orange (eruption occurring within days to weeks). Nevado del Ruiz had two minor explosive eruptions in May and June 2012 (Volcanic Explosivity Index [VEI] = 1; Fig. 2). These eruptions were low in energy with eruption columns less than 10 km high above the summit crater of the volcano. The eruption generated small lahars, which impacted the area proximal to the volcano and did not cause any loss of human lives. Proper risk management allowed the SGC-OVSM to successfully manage the crisis. After the 2012 eruptions, Nevado del Ruiz remained in a state of unrest with volcano-tectonic earthquakes, discharges of water vapor, SO_2 and ash, and inflation of the volcanic edifice (Servicio Geológico Colombiano, 2012). In August 2015, magma moved to the surface and a lava dome began to be emplaced at the bottom of the crater floor (Fig. 2). The dome continued to grow for several months, reaching a diameter of approximately 130 m, an estimated maximum height of 60 m (Kósik et al., 2015). The upper half of the dome (i.e., the dome visible above the crater floor) had a volume of $1.1 \pm 0.2 \times 10^6$ m^3 in December 2019. Seismicity and gas/ash discharges kept ongoing until 2021, while deformation had already stopped at the beginning of 2018.

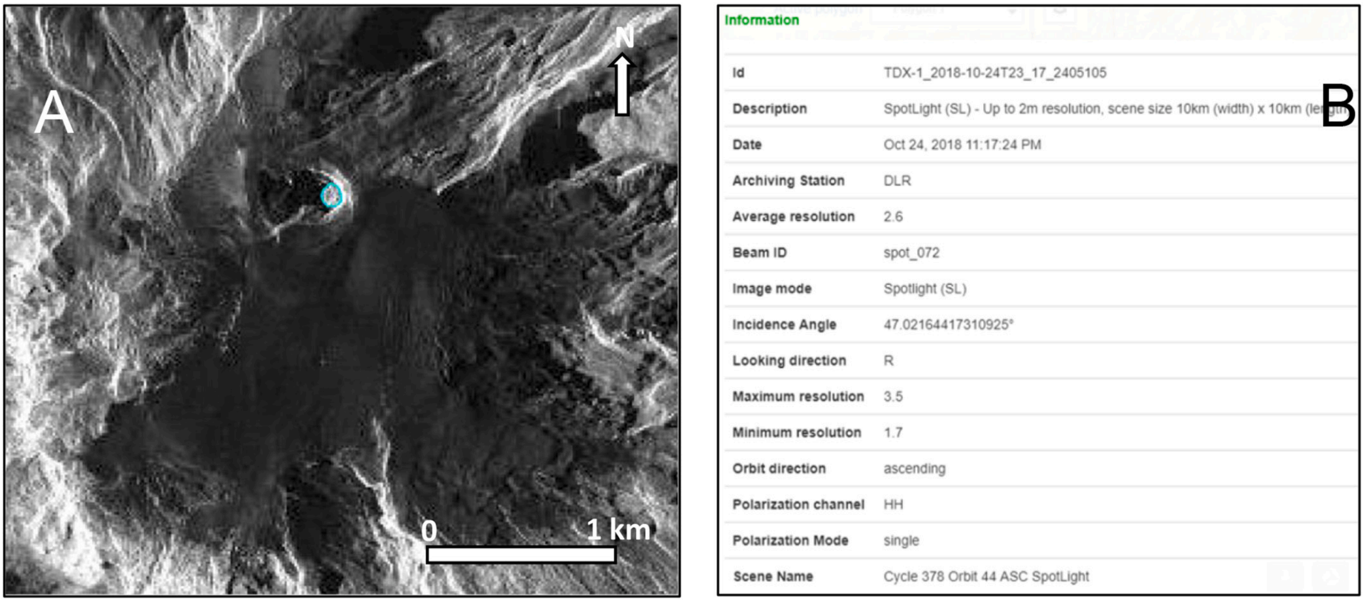

Fig. 8. (A) TanDEM-X radar Image of Nevado del Ruiz taken on October 24, 2018, at 11:17 pm (local time). The blue polygon represents the perimeter of the lava dome. (B) Metadata of the TanDEM-X radar Image. (For interpretation of the references to colour in this figure legend, the reader is referred to the web version of this article.)

4. The lava dome

4.1. Morphology

Two years after the end of the dome forming eruption, the estimated minor/major diameter of the crater was ~930/980 m, respectively, and its depth about 300 m (measurements made in January 2020; Figs. 3, 4, and 5). There were still minor terraces limited by steps. There was no longer a glacier, or snow deposits, inside and close to the crater (Fig. 3) because of the unrest, the latest eruptions, and the effects of climate change on the summit glacier (Ceballos et al., 2020b; IPCC, 1997).

Since 2015, fumarolic vents of water vapor, sulfur dioxide (SO_2) and ash have been active at the bottom of the crater. The fumaroles mark the contour of a volcanic conduit of approximately 200 m in diameter. This zone represents an area of structural weakness of the crater, where the new lava dome is emplaced (Figs. 3, 4, and 5).

The diagram in Fig. 5 offers a summary of the main features of the volcano summit and Arenas crater deduced from the images in Figs. 3, 4, and 6, while Fig. 7 shows thermal images of the crater from the Sentinel-2 satellite.

4.2. Dome growth and extrusion rate

Thirty-seven TanDEM-X (TDX) and thirty TerraSAR-X (TSX) images from the German Aerospace Center (https://terrasar-x-archive.terrasar.com) were processed to monitor the dome growth and extrusion rate (Hale et al., 2009). To standardize accuracy, we used images with the same characteristics: SpotLight mode, up to 2.5 m horizontal resolution, a 10 km × 10 km scene size, taken at nighttime (around 11 P.M.- local time), ascending path direction, and 47 degrees of incidence angle (Fig. 8).

4.3. Perimeter, surface area, and volume of the lava dome

To estimate the total volume of the dome, we divided the dome in two sections: upper half and lower half dome (e.g., Valenzuela, 2011; Fig. 9).

To estimate of the surface area and volume of the upper half dome, the one above the bottom of the crater (Fig. 9), we first scaled and georeferenced the radar amplitude signal of the TDX and TSX images. We chose the Planet Labs image of March 14, 2018 (Fig. 10A), showing a clear view of the bottom of the crater, to calibrate the initial dimensions of the dome. These dimensions were assumed equivalent to the dimensions of the dome in the TDX image of April 9, 2018 (Fig. 10B). Using this calibration, we estimated a pixel per meter factor of 16.9 pixel/m and applied it to all images. Then we digitized a border polygon in each image to calculate the perimeter and the surface area of the dome (Fig. 10C and 10D). Finally, we estimated the height of the dome, and we applied the formula for an oblate ellipsoid half-dome (Monolithic Dome Institute, 2001) to calculate the volume of the upper section of the dome (Kósik et al., 2015).

The upper half of the dome reached its maximum surface area ($5 \pm 1 \times 10^4$ m^2) and maximum volume ($1.1 \pm 0.2 \times 10^6$ m^3) on December 5, 2019 (Fig. 11). The estimated error for the surface area and volume of the dome is ~20% since the measurements of the polygon edges were obscured by ash deposits and the low resolution of the images. The images at the end of 2020 and beginning of 2021 show a decrease in the volume of the lava dome to $0.9 \pm 0.2 \times 10^6$ m^3, probably because of the erosion of the flank edges of the dome by small explosions and constant emission of ash (Fig. 11). The lava extrusion rate reached its maximum twice. At the beginning of the extrusion process, a short-lived pulse of ~0.19 m^3/s in November 2015, and a second lasting most of 2016. The lava extrusion rates declined abruptly to 0.02 m^3/s in February 2018. The negligible volume of lava extrusion since February 2019 marked the end of any significant growth of the lava dome (Fig. 11).

We estimated the volume of the lower section of the dome using a plane located below the upper section in contact with the perimeter of 10-m resolution DEMs of the Arenas crater. The volume obtained from the DEM of the Alos Palsar-1 image is $0.63 \pm 0.10 \times 10^6$ m^3, while the volume obtained from the DEM of the TerraSAR-X image is $0.62 \pm 0.10 \times 10^6$ m^3 (Fig. 9). The total volume of the dome, obtained adding the volume of the upper and lower sections, is of $1.7 \pm 0.2 \times 10^6$ m^3.

5. Simulation of dome extrusion

We simulated the lava dome extrusion using the LAVA-C code developed by the Geoscience Group of University of South Florida (USF; Richardson and Connor, 2014). The code algorithm simulates the

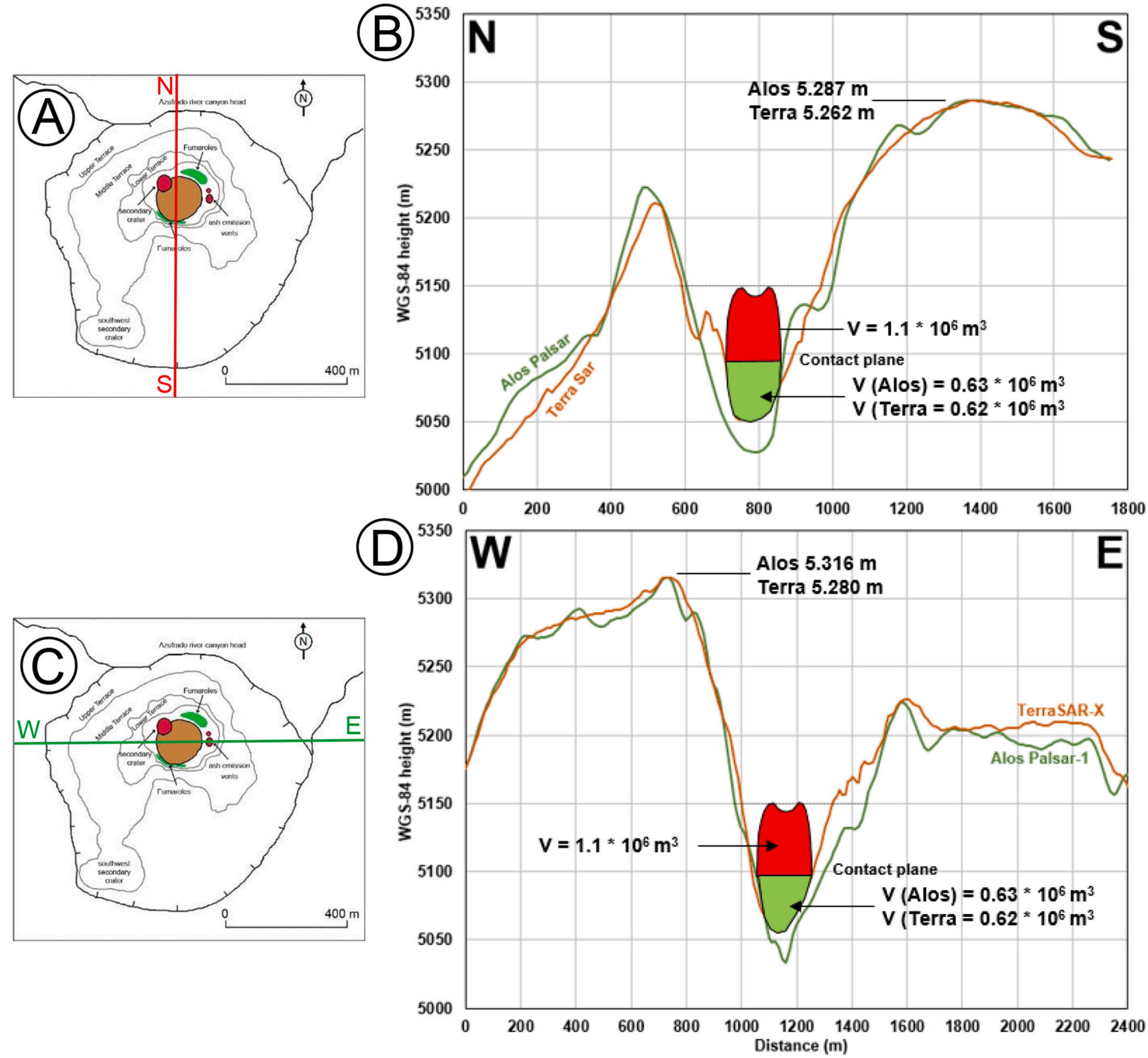

Fig. 9. Profiles of the summit of Nevado del Ruiz and the Arenas crater extracted from DEMs built from TerraSAR-X and Alos Palsar-1 images.(A) Map of the Arenas crater with a North-South section (Red line); (B) North-South profile; (C) Map of the Arenas crater with a West-East section (Green line); and (D) West-East profile. The maximum heights of the summit (datum WGS-84 ellipsoid) measured on both DEMs are 5280 m (TerraSAR-X) and 5316 m (Alos) respectively. The red areas represent the upper section of an oblate ellipsoid half-dome (estimated volume: $1.1 \pm 0.1 \times 10^6$ m^3). The green areas represent the lower section inferred from the DEMs (estimated volumes: Alos Palsar-1, $0.63 \pm 0.10 \times 10^6$ m^3; TerraSAR-X, $0.62 \pm 0.10 \times 10^6$ m^3). The dome total volume is obtained adding the upper and lower sections ($1.7 \pm 0.2 \times 10^6$ m^3). The height of the upper section is 60 m (height of the dome). The height of the lower section is estimated based on the DEMs. (For interpretation of the references to colour in this figure legend, the reader is referred to the web version of this article.)

extrusion of a lava dome through pulses of lava assuming a semi-empirical relation between a reference thickness and the viscosity of the lava. The code requires a DEM of the volcano's crater to estimate the changes in slope and constrain the thickness of the lava pulses. For the simulations, we used the 10 m-per-pixel DEM of Nevado del Ruiz from USF (Deng et al., 2019), associated the location of the extrusion vent with the approximated centroid of the lava dome observed in the images of Nevado del Ruiz, and assumed a lava pulse of 56.5×10^5 m^3, i.e., the monthly mean of the total dome volume.

We ran 120 simulations using different volume limits between 0.5 and 1.5×10^6 m^3 (Fig. 12). A volume of $1.05 \pm 0.20 \times 10^6$ m^3 yields the best fit between the dome's perimeter and the height of its upper half section (e.g., Fig. 9).

6. Lava dome dem's and photogrammetric mosaics

We created two Digital Elevation Models (DEMs) of Arenas crater (Fig. 13), and two photogrammetric 3D mosaics of the lava dome (Fig. 14) to illustrate the evolution of the dome forming eruption.

The DEMs are based on an image of January 1st, 2015, from TerraSAR and Alos Palsar data, when the dome was not present (Fig. 13, A), and an image of March 28, 2018, again from TerraSAR and Alos Palsar

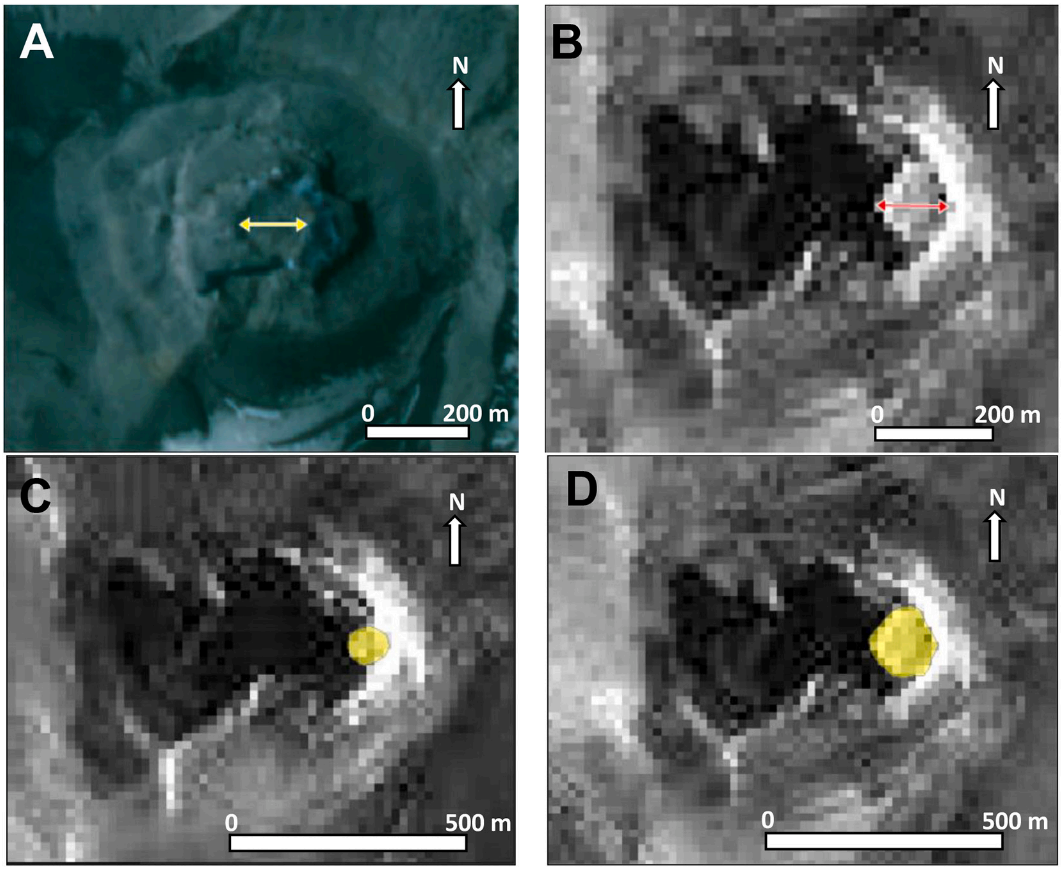

Fig. 10. Diagram of the methodology employed to calculate the surface area and volume of the lava dome. (A) scaling of image from the Planet Labs image of March 14, 2018 (image courtesy of Planet Labs FBC, available online at https://www.planet.com); (B): scaling from TDX image (April 9, 2018); (C): example of digitized dome border polygon, TDX image of November 11, 2015; (D) example of digitized dome border polygon, TDX image of May 25, 2018.

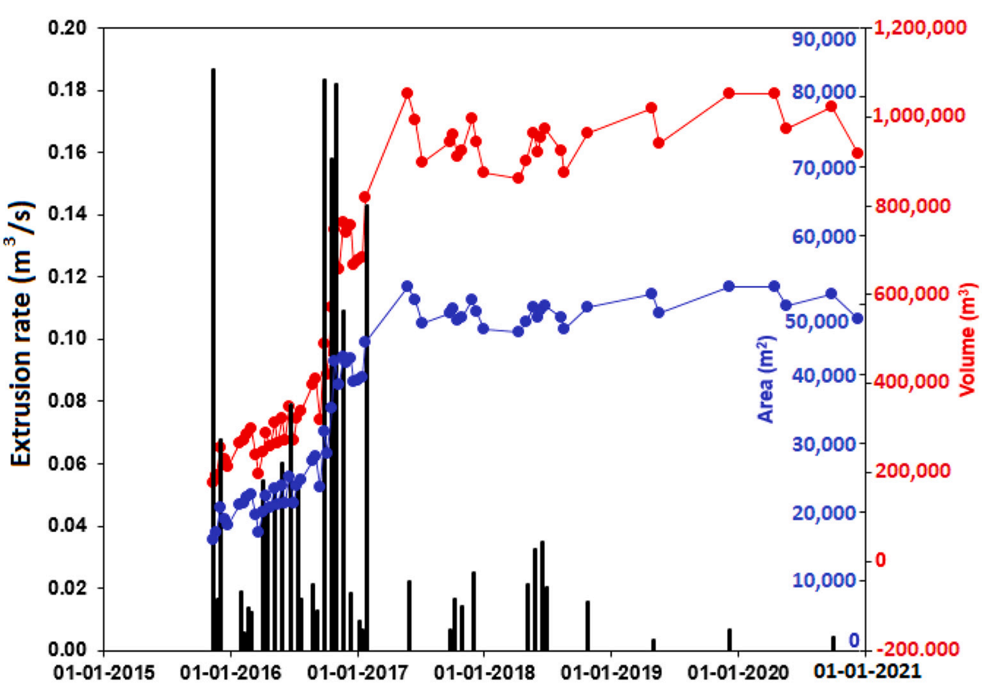

Fig. 11. Lava dome growth at Nevado del Ruiz: time series of volume (red line), surface area (blue line) and lava extrusion rate (black bars) from November 2015 to January 2021. Two peaks in lava extrusion rate were detected: a first short-lived pulse in November 2015 (~0.19 m^3/s) and a second lasting most of 2016. The lava extrusion rates declined abruptly to ~0.02 m^3/s in February 2018. The negligible volume of lava extrusion since February 2019 marked the end of the dome forming eruption. (For interpretation of the references to colour in this figure legend, the reader is referred to the web version of this article.)

data, when the lava dome was present (Fig. 13, B).

We created the photogrammetric 3D mosaics of the dome from aerial photographs of January 10 of 2020 (Fig. 14, A) and January 29, 2021 (Fig. 14, B; photos courtesy of Jerónimo Valencia). Both mosaics are projected on the 10 m-per-pixel DEM by University of Southern Florida (USF, Deng et al., 2019).

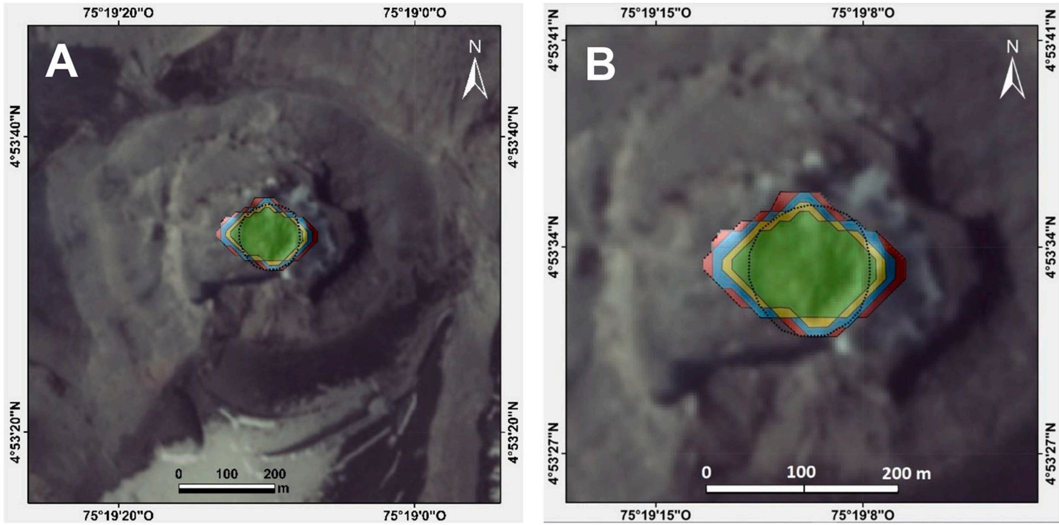

Fig. 12. Simulation of dome extrusion. The background is the Planet Labs image of March 14, 2018 (Image courtesy of Planet Labs FBC, available online at https://www.planet.com). (A) View of the Arenas crater and the dome in the bottom (Black dotted line) with the overlapping polygons resulted from the simulations. (B) Detail of the simulation polygons results for volumes of 800,000 m^3 (green), 1,050,000 m^3 (yellow), 1,300,000 m^3 (blue), and 1,500,000 m^3 (red). The dome border is represented by the black dotted line. (For interpretation of the references to colour in this figure legend, the reader is referred to the web version of this article.)

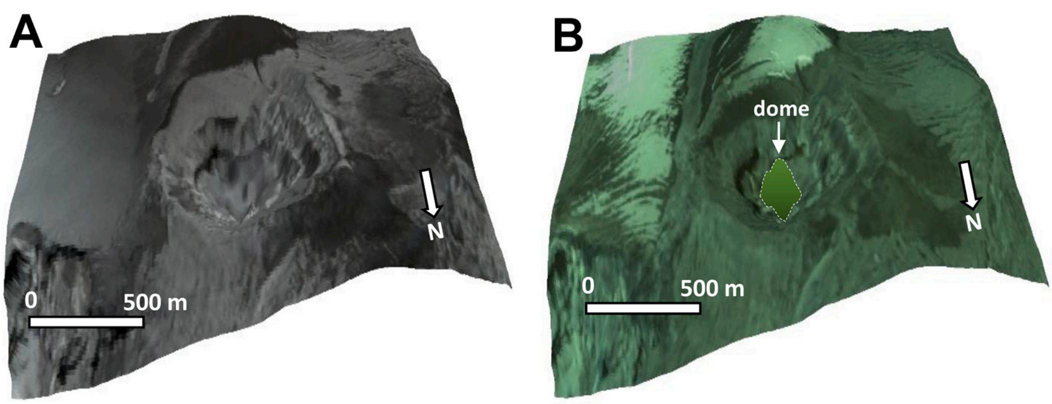

Fig. 13. Digital Elevation Models (DEMs) of the Arenas crater (Nevado del Ruiz). (A) DEM created from the image of January 1st of 2015, the dome forming eruption began in August 2015. (B) DEM from the image of March 28, 2018, showing the lava dome at the bottom of the crater. The dome is based on the 10 m-per-pixel DEM by USF (Deng et al., 2019).

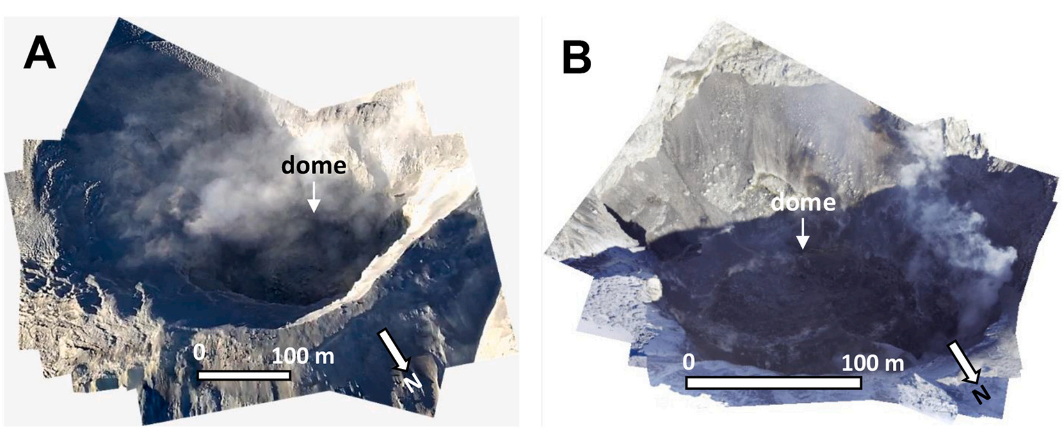

Fig. 14. Photogrammetric 3D mosaics of Arenas crater and the lava dome. (A) Mosaic from aerial photographs of January 10 of 2020. (B) Mosaic from aerial photographs of January 29, 2021 (images courtesy of Jerónimo Valencia). Both mosaics are built on the 10 m-per-pixel DEM by USF (Deng et al., 2019).

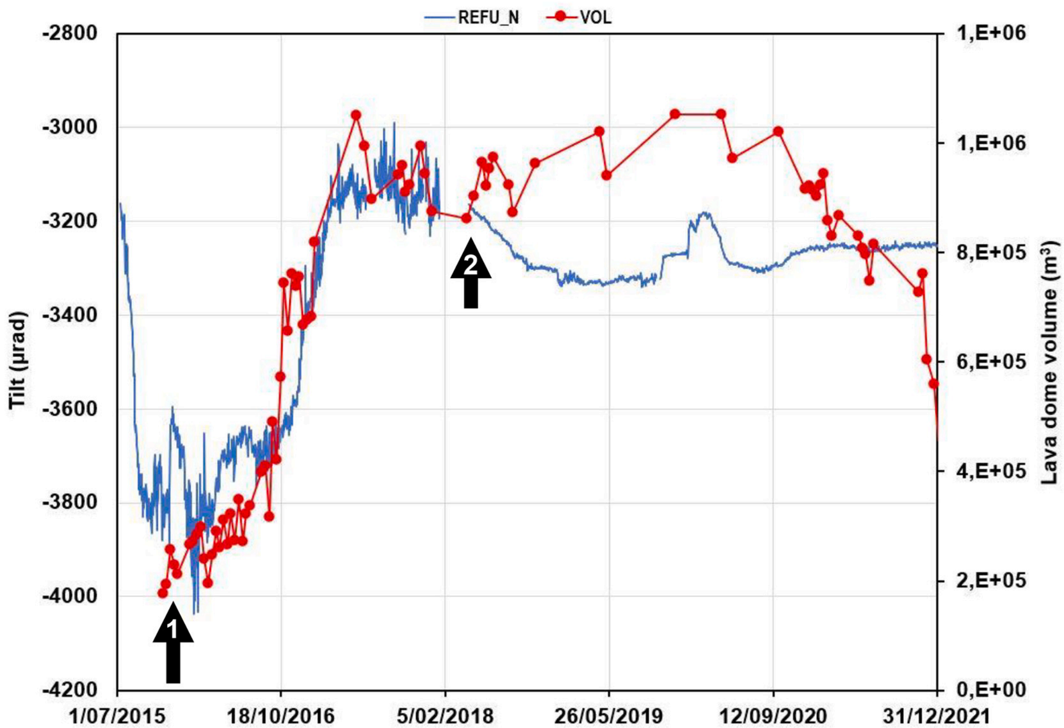

Fig. 15. Time series of changes in the volume of the lava dome (red line and markers) and the mirror image of the north tilt component of the tiltmeter Refugio (blue line) between July 2015 and December 2020. Black arrow (1): Initial pick of tilt (November 2015) and beginning of the dome forming eruption. Black arrow (2): Beginning of the slow decay of the tilt signal and of the end of the dome forming eruption (September 2017). (For interpretation of the references to colour in this figure legend, the reader is referred to the web version of this article.)

7. Dome growth from geodetic measurements

The correlation between deformation and dome growth is shown in Fig. 15. Precursory aseismic deflation was observed in the tiltmeters and GNSS stations between 2009 and late 2011 (Fig. 2). Inflation of the volcanic edifice began between January and February 2012 and lasted until the beginning of 2018 (see NEREIDAD GNSS time series in Fig. 2). The tiltmeter REFUGIO, located at 2.3 km northwest of Arenas crater, at an altitude of 4800 m a.s.l. (the height of the volcano is 5231 m a.s.l.) (Fig. 1), recorded an initial peak of maximum tilt in November 2015 and a second peak in March 2016 (Fig. 2 and Fig. 15). An inflation trend of almost 10 cm was detected using differential interferometric synthetic aperture radar observations (DinSAR) from mid-2011 to end-2014 (Lundgren et al., 2015; Fig. 2). The deformation recorded in the tiltmeters, GNSS stations and InSAR is correlated to the migration of magma and dome forming eruption. The tilt changes measured by the tiltmeter REFUGIO (Fig. 15), and the time series of the vertical deformation recorded by the GNSS site NEREIDAS (Fig. 1 and Fig. 2) illustrate the slow, but continuous discharge of magma feeding the lava dome.

The time series of the volume change of the lava dome (Fig. 15, red line) and the specular image of the time series of the north tilt component of the tiltmeter REFUGIO (Fig. 15, blue line) show a correlation between the deformation of the volcanic edifice and the changes in the volume of the lava dome (Fig. 15). The initial peak of maximum tilt occurred in November 2015, coinciding with the initial lava emplaced at the bottom of the Arenas crater (Fig. 15). Tilt and the volume of the lava dome increased until February 2018. Since March 2018, the tilt has been slowly decaying, marking the beginning of the end of the dome-forming eruption (Fig. 15).

8. Summary and conclusions

Summit observations of Nevado del Ruiz were conducted between 1939 and the 1984 by climbers. These observations allow a qualitative reconstruction of the morphology of Arenas crater and the evolution of the fumarolic activity (see Supplementary Material).

INGEOMINAS (now Colombian Geological Survey - SGC) started an instrumental monitoring program in 1985 that has evolved to include GNSS, tiltmeters, aerial photography and InSAR (Ordoñez et al., 2015).

Using radar images, aerial photographs, and geodesy, we have been able to document the beginning of the extrusion of the lava dome in August 2015, infer its evolution and volume change between 2015 and 2021, and estimate its total volume, $1.7 \pm 0.2 \times 10^6$ m^3 (Fig. 11 and Fig. 9). Two peaks in lava extrusion rate were detected: a first short-lived pulse in November 2015 ($\sim$0.19 m^3/s) and a second lasting most of 2016 (Fig. 11). The lava extrusion rates declined abruptly to $\sim$0.02 m^3/s in February 2018. The decay in the tilt signal in February 2018 marked the beginning of the end of the dome forming eruption. The negligible volume of lava extrusion since February 2019 denoted the practical end of the dome forming eruption (Figs. 11 and 15).

Remote sensing images from TanDEM-X and TerraSAR-X provided an effective means to track and quantify the dome growth at Nevado del Ruiz. The radar images permitted an estimate of the average volumes of magma-intrusion and discharge rates of the dome-forming eruption with an error of $\sim$20% (Figs. 8, 10, and 11). These images are inexpensive compared with the excessive costs of aerial photographs, or high-resolution scans from aerial/terrestrial lidar, and provide an alternative for volcanoes located in areas where weather conditions can limit direct observations. Finally, we were able to infer a strong correlation between dome growth and summit deformation (Fig. 15).

Together with instrumental monitoring, the direct observation of changes in the volcano's morphology (see Supplementary Material) reminds authorities and local communities that the Nevado del Ruiz is active and represents a serious hazard. Direct observation, although qualitative, remains critical since the local culture stresses the importance of oral traditions and practical experience. The direct representation by pictures and maps of changes in the morphology of Arenas's crater, like the evolution of the fumarolic activity, formation of ponds, and disappearance of ice deposits allows effective communication with local communities about the hazard represented by the volcano. Open communication with the communities living around and close to Nevado del Ruiz is the key component of an effective management and reduction of the volcanic risk.

Author contributions

Bibliographic compilation, M.O. and C.L.; photographs, maps edition, manuscript writing—original draft preparation, resources, project supervision, and data curation, M.O.; data processing, and modeling, C. L. and M.O.; software, C.L.; conceptualization, manuscript writing—final review and editing, M.O. and M.B.; advising, funding, M.B.; analysis of observations, and geomorphological evolution and interpretation, M. O.; all authors have read and agreed to the published version of the manuscript.

Funding

This work was funded by the Colombian Geological Survey and supported by the Colombian Air Force. Additional funding for this work came from USAID via the Volcano Disaster Assistance Program, from the U.S. Geological Survey Volcano Hazards Program, and from Sapienza–University of Rome, Piccoli Progetti Universitari 2020.

Declaration of Competing Interest

The authors declare no conflict of interest.

Acknowledgments

We thanks Diego Lozada, Guillermo Sanchez, Guillermo Cajiao, Héctor Mora, Instituto Geográfico Agustín Cadazzi-IGAC, Jair Ramirez, Jerónimo Valencia, Manizales History Center, Marta Calvache, and the SGC-OVSM archive section for providing photographs and the permission to use them in this paper. We thank Europe Space Agency, Planet Labs Inc. and German Aerospace Center for providing remote sensing images. Constructive comments and suggestions by Chris Harpel (USGS), Boris Behncke (INGV), Kelly Russell (UBC) and Sonia Calvari (Editor) helped to improve the manuscript. Any use of trade, firm, or product names is for descriptive purposes only and does not imply endorsement by the U.S. Government.

Appendix A. Supplementary data

Supplementary data to this article can be found online at https://doi.org/10.1016/j.jvolgeores.2022.107626.

References

Blake, S., 1990. Viscoplastic models of lava domes. In: Fink, J.H. (Ed.), Lava Flows and Domes. Springer, Berlin, Heidelberg, pp. 88–126. https://doi.org/10.1007/978-3-642-74379-5_5.

Ceballos, J.L., Martínez, L.M., Valencia, L.G., Pulgarín, B.A., Correa, A.M., Narváez, B.L., 2020a. Geological evolution of the Nevado del Ruiz Volcanic Complex. In: Gómez, J., Pinilla, A.O. (Eds.), The Geology of Colombia, Volume 4 Quaternary. Servicio Geológico Colombiano, Publicaciones Geológicas Especiales, 38. Bogotá, pp. 267–296. https://doi.org/10.32685/pub.esp.38.2019.07.

Ceballos, J.L., Ospina, J.A., Rojas, F., 2020b. Informe del estado de los glaciares colombianos 2019. Grupo de Suelos y Tierras, IDEAM. Bogotá, Colombia. Internal report, p. 28 available on line at. http://www.ideam.gov.co/documents/11769/229819/Estado+de+los+glaciares+colombianos+2019/0fdd1967-28bd-4120-9d58-8ebe81deaf8c.

Deng, F., Rodgers, M., Xie, S., Dixon, T., Charbonnier, S., Gallant, E., López, C., Ordoñez, M., Malservisi, R., Voss, N., Richardson, J., 2019. High-resolution DEM generation from spaceborne and terrestrial remote sensing data for improved volcano hazard assessment - a case study at Nevado del Ruiz, Colombia. Remote Sens. Environ. 233, 111348 https://doi.org/10.1016/j.rse.2019.111348.

Drusch, M., Del Bello, U., Carlier, S., Colin, O., Fernandez, V., Gascon, F., Hoersch, B., Isola, C., Laberinti, P., Martimort, P., Meygret, A., Spoto, F., Sy, O., Marchese, F., Bargellini, P., 2012. SENTINEL-2: ESA's Optical High-Resolution Mission for GMES Operational Services. Remote Sens. Environ. 120, 25–36. https://doi.org/10.1016/j.rse.2011.11.026.

Fink, J., Anderson, S., 2000. Lava domes and coulees. In: Encyclopedia of Volcanoes. Academic Press, London, pp. 307–319.

Hale, A.J., Calder, E.S., Wadge, G., Loughlin, S.C., Ryan, G.A., 2009. Modelling the lava dome extruded at Soufrière Hills Volcano, Montserrat. August 2005-May 2006: part I: Dome shape and internal structure. J. Volcanol. Geotherm. Res. 187, 53–68. https://doi.org/10.1016/j.jvolgeores.2009.08.023.

INGEOMINAS, 2010. Boletín semestral de actividad registrada por los volcanes activos del complejo volcánico Cerro Bravo – Cerro Machín. Internal report, p. 104 in Spanish, available on line at. https://www2.sgc.gov.co/Publicaciones/Informes%20tcnicos/Informe%20t%C3%A9cnico%20del%20segundo%20semestre%20de%202010.pdf.

IPCC, 1997. Grupo Intergubernamental de Expertos sobre el Cambio Climático. Impactos regionales del cambio climático: evaluación de la vulnerabilidad. (Incluido en resumen para responsables de políticas). In: Informe especial del Grupo de trabajo II del IPCC, 1997. ISBN: 92–9169–310-3, in Spanish available online at. https://archive.ipcc.ch/pdf/special-reports/spm/region-sp.pdf.

Jarvis, A., Guevara, E., Reuter, H.I., Nelson, A.D., 2008. Hole-Filled SRTM for the Globe: Version 4 Data Grid Available from the CGIAR-CSI SRTM 90m Database. CGIAR Consortium for Spatial Information, Available online at. http://srtm.csi.cgiar.org.

Kósik, S., Nemeth, K., Procter, J., Kereszturi, G., Cronin, S., 2015. DEM-based analysis of the morphometry of lava domes; a case study from the Taupo Volcanic Zone, New Zealand. Poster 26, IUGG Assembly 2015, Prague. Available online at. https://www.researchgate.net/publication/279298974.

Lundgren, P., Samsonov, S.V., López, C.M., Ordoñez, M., 2015. Deep source model for Nevado del Ruiz Volcano, Colombia, constrained by interferometric synthetic aperture radar observations. Geophys. Res. Lett. 42, GL063858. https://doi.org/10.1002/2015GL063858.

Monolithic Dome Institute, 2001. Spherical Dome Formulas – Ellipsoid Dome Formulas. Monolithic Dome Institute. Available online at. http://static.monolithic.com/pdfs/formulas.pdf (accessed 10/18/2021).

Ordoñez, M., López, C., Alpala, J., Narváez, L., Arcos, D., Battaglia, M., 2015. Keeping Watch over Colombia's Slumbering Volcanoes, EOS, 96, February 2015. https://doi.org/10.1029/2015EO025079.

Richardson, J., Connor, L., 2014. Lava C Version 0.1. Available online at. https://vhub.org/resources/3597.

Servicio Geológico Colombiano, 2012. Informe de actividad volcánica Segmento Norte de Colombia complejo volcánico (Cerro Bravo-Cerro Machín) 2012. Internal report, 96 pp., in Spanish. available on line at. https://www2.sgc.gov.co/Publicaciones/Informes%20tcnicos/Informe%20t%C3%A9cnico%20anual%20de%202012.pdf.

Servicio Geológico Colombiano, 2015. Informe de actividad volcánica Segmento Norte de Colombia Agosto de 2015. Internal report, 86 pp., in Spanish. available on line at. https://www2.sgc.gov.co/Publicaciones/Informes%20tcnicos/Informe%20del%20mes%20de%20agosto%202015.pdf.

Valenzuela, C.E., 2011. Tasa de crecimiento del complejo de domos del Volcán Chaitén, periodo mayo 2008 - diciembre 2009. Universidad de Chile, Facultad de Ciencias Físicas y Matemáticas, Departamento de Geología, undergraduate thesis, 63 pp., in Spanish. available online at. http://repositorio.uchile.cl/handle/2250/104343.

Voight, B., 1990. The 1985 Nevado del Ruiz volcano catastrophe: anatomy and retrospection. J. Volcanol. Geotherm. Res. 42, 151–188. https://doi.org/10.1016/0377-0273(90)90075-Q.